Modeling of High-Pressure Ethylene Polymerization. I. Kinetic Parameters of Oxygen Initiation

B. CERINSKI,[1] J. JELENCIC[2]

[1] Korculanska 1., 10000 Zagreb, Croatia

[2] Faculty of Chemical Engineering and Technology, 10000 Zagreb, Croatia

Received 15 November 2000; accepted 11 June 2001

ABSTRACT: A kinetic model of a high-pressure, free-radical ethylene polymerization is presented. The model of S. Goto, K. Yamamoto, S. Furui, and M. Sugimoto (J Appl Polym Sci, Appl Polym Symp 1981, 36, 21), developed for several common peroxides, was extended to be applicable for the oxygen initiation also. Small-extent propylene copolymerization, as well as telomerization with isobutane and propylene, are included into the overall kinetic scheme. The model is based on a string of elemental continuously stirred tank reactors and is particularly suited for the tubular low-density polyethylene reactors. © 2002 John Wiley & Sons, Inc. J Appl Polym Sci 83: 2043–2051, 2002

Key words: ethylene polymerization; mathematical model; tubular reactor

INTRODUCTION

In the past thirty years, numerous mathematical models of ethylene free-radical polymerization have been published.[1,2] They differ in respect to the reactor's model applied, initiator(s) and telomer(s) used, kinetic peculiarities, etc. Although the oxygen is among the most frequently used initiators, the majority of models pertained to the peroxide initiation of low-density polyethylene (LDPE) production in tubular reactors. Only the article of Brandolin et al.[3] deals with oxygen-initiated polymerization in a tubular reactor. Unfortunately, this model was developed solely for oxygen initiation and a single injection reactor, being therefore inapplicable for the more complex design of the contemporary reactors.

At the present time, a vast number of high-pressure tubular LDPE reactors operate as multi-injection, mixed initiators. They are directed by higher demands, considering the cost, quality, and safety the plants are faced with. Computer aids in a plant information/control system, model-based simulation, and wide application of statistics are commonly accepted. The models have become an important tool in the many engineering tasks.

The objective of this work was to give a mathematical model for any tubular reactor design. It was desirable for the model to be simple and easy for computer implementation. An integration of an oxygen-initiated process with an appropriate model for the peroxide-initiated one seemed good for this purpose. The model of Goto et al.,[4] developed for several common peroxides, was chosen to be a convenient one for this extension. This model was taken as a master model. Being fully reproducible, with a comprehensive kinetic scheme, computer implementation was simple at the same time.

Experimental data, obtained from several industrial LDPE plants, operating with oxygen ini-

Correspondence to: B. Cerinski.

Journal of Applied Polymer Science, Vol. 83, 2043–2051 (2002)

DOI 10.1002/app.10106

Table I Kinetic Parameters of Initiation for Several Common Peroxides[4]

Species	k's	A (s^{-1})	E (J/mol)	Δv (cm^3/mol)
TBPV	k_i	1.63×10^{14}	118,000	2.5
	k_x	1.66×10^{25}	214,000	0.0
TBIB	k_i	1.05×10^{15}	132,000	2.5
	k_x	5.17×10^{28}	257,000	0.0
TBPC	k_i	1.42×10^{15}	141,000	2.5
	k_x	2.03×10^{27}	259,000	0.0
DTBP	k_i	6.64×10^{15}	156,000	2.5
	k_x	2.04×10^{28}	284,000	0.0
DCP	k_i	1.12×10^{18}	170,000	2.5
	k_x	1.41×10^{30}	289,000	0.0

TBPV, *t*-butyl peroxypivalate; TBIB, *t*-butyl perisobutylate; TBPC, *t*-butyl perisopropylcarbonate; DTBP, di-*t*-butyl peroxide; DCP, dicumyl peroxide.

tiation, were used for additional kinetic parameter derivation. A very good match between experimental and computed reactors' performances was achieved.

KINETIC SCHEME

Kinetic scheme of the master model includes other elemental processes:

1. Peroxide initiation:

$$I \rightarrow 2R_1 \quad k_i \tag{A}$$

$$I \rightarrow X \quad k_x \tag{B}$$

2. Propagation:

$$M + R_m \rightarrow R_{m+1} \quad k_p \tag{C}$$

3. Intramolecular transfer:

$$R_m \rightarrow R_m \quad k_b \tag{D}$$

4. Transfer to telomer(s):

$$T + R_m \rightarrow P_m + R_1 \quad k_{t1} \tag{E}$$

5. Transfer to polymer:

$$R_m + P_n \rightarrow P_m + R_n \quad k_{tp} \tag{F}$$

6. Termination:

$$R_m + R_n \rightarrow P_n + P_m/P_{m+n} \quad k_t \tag{G}$$

7. β_1 scission:

$$R_{m+n} \rightarrow P_n + R_m \quad k_{\beta 1} \tag{H}$$

8. β_2 scission:

$$R_{m+n} \rightarrow P_n + R_m \quad k_{\beta 2} \tag{I}$$

Kinetic parameters adopted from the master model are summarized in Tables I and II.

The additional elemental reactions are introduced to extend the model application to the oxygen initiation.

9. Oxygen initiation:

$$O_2 \rightarrow 2R_1 \quad fk_{O_2} \tag{A1}$$

10. Thermal initiation:

$$C_2H_4 \rightarrow R_1 \quad k_{ti} \tag{A2}$$

and to a small extent, copolymerization with α-olefins.

11. Copolymerization with propylene (Pr):

$$P_r + R_m \rightarrow R_{m+1} \quad k_{co} \tag{J}$$

Initiator effectiveness factor $f \leq 1$ is introduced in step (A1) as it is frequently done in a numerous models.[2] These additional parameters are summarized in Table III.

Table II Kinetic Parameters of the Master Model[4]

Process	A (dm^3/mol s or s^{-1})	E (J/mol)	Δv (cm^3/mol)
k_p	1.56×10^8	44,000	−19.7
k_b	1.02×10^9	54,500	−23.5
$k_{tl}(C_6)$	3.42×10^7	53,600	−19.5
k_{tp}	4.86×10^8	58,900	4.4
k_t	8.33×10^7	12,600	13.0
$k_{\beta 1}$	1.62×10^8	65,900	−22.6
$k_{\beta 2}$	2.36×10^7	60,800	−19.7

Table III Kinetic Parameters for Oxygene Polymerization

Process	A (dm^3/mol s or s^{-1})	E (J/mol)	Δv (cm^3/mol)
f (≤ 1)	8.20×10^{-10}	−84,000	47.0
k_{O_2}	6.00×10^{9}	116,000	0.0
k_{ti}	7.80	151,000	−168
k_{co} (C_3^-)	4.82×10^{10}	73,000	−19.5
k_{tl} (C_3^-)	1.34×10^{10}	73,000	−19.5
k_{tl} (i − C_4)	1.34×10^{10}	73,000	−19.5

Kinetic constants, k's, and effectiveness factor, f, are expressed in the usual form of the Arrhenius equation:

$$k = A \exp(-(E + P\Delta v)/\mathrm{RT}) \tag{1}$$

Pressure, P, should be taken in MPa. Rate equations which constitute the model are as follows:

$$r_i(R) = 2k_iC_i \tag{2}$$

$$r_i(I) = -(k_i + k_x)C_i \tag{3}$$

$$r_p(M) = -k_pC_mC_r \tag{4}$$

$$r_b(R) = k_bC_r \tag{5}$$

$$r_{t1}(T) = -k_{t1}C_{t1}C_r \tag{6}$$

$$r_{tp}(P) = k_{tp}C_rC_p \tag{7}$$

$$r_t(P) = k_tC_r^2 \tag{8}$$

$$r_{\beta 1}(R) = -k_{\beta 1}C_r \tag{9}$$

$$r_{\beta 2}(R) = -k_{\beta 2}C_r \tag{10}$$

$$r_{O_2}(\mathrm{O}) = -k_{O_2}C_{O_2} \tag{11}$$

$$r_{O_2}(R) = 2fk_{O_2}C_{O_2} \tag{12}$$

$$r_{ti}(R) = k_{ti}C_m \tag{13}$$

$$r_{co}(\mathrm{Pr}) = -k_{co}C_{pr}C_r \tag{14}$$

All radicals (R_1, R_m, and R_n) are represented by the symbol R in the encountered rate equations.

Quasy steady state assumption (QSSA)[5] was formulated on the equality of rates of radical generation and depletion. In the model of peroxide initiation, QSSA is expressed as,

$$2k_iC_i = k_tC_r^2 \tag{15}$$

The concentration of free radicals is the given by,

$$C_r = (2fk_iC_i/k_t)^{1/2} \tag{16}$$

Similar expressions can be written for the oxygen initiation:

$$2fk_{O_2}C_{O_2} + k_{ti}C_m = k_tC_r^2 \tag{15a}$$

$$C_r = ((2fk_{O_2}C_{O_2} + k_{ti}C_m)/k_t)^{1/2} \tag{16a}$$

QSSA greatly simplifies the computation procedure.

FUNDAMENTALS OF THE REACTOR MODELING

A series of elemental continuous stirred tank reactors (CSTRs) was chosen for the tubular reactor modeling. Figure 1 schematically shows this arrangement.

A simpler case of a multi-injection tubular reactor (i.e., single initiator/single telomer use) is depicted. Molar flow rates of the monomer, initiator, and telomer (F_m, F_i, and F_{tl}) enter the first CSTR at the reactor's inlet pressure, P, and temperature, T. The conversions of these species are given, respectively, by the equations[6]:

$$X_m = -r_p(M)V/F_{m,\mathrm{in}} \tag{17}$$

$$X_i = -r_i(I)V/F_{i,\mathrm{in}} \tag{18}$$

$$X_{t1} = -r_{t1}(T)V/F_{tl,\mathrm{in}} \tag{19}$$

Obviously, for multi-initiation/multitelomerization and copolymerization processes, the set of equations is larger. In the case of oxygen initiation and a small extent propylene copolymerization/telomerization, the conversions are given by,

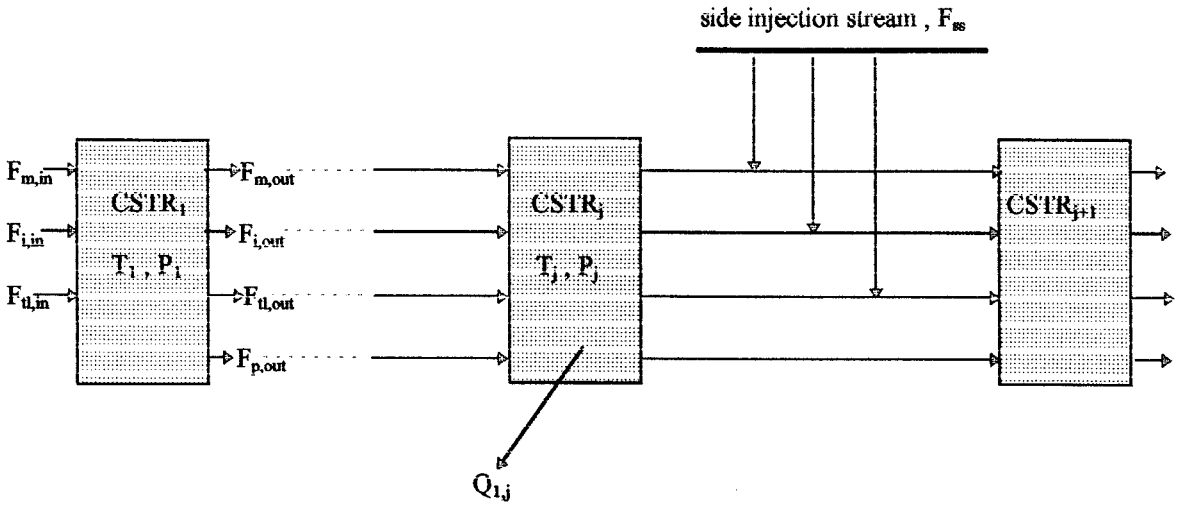

Figure 1 Schematic representation of a tubular LDPE reactor by the series of elemental CSTRs; F, molar flow rates of the inlet (in) and outlet (out) streams of the species: monomer (m), initiator (i), telomer (tl), and polymer (p).

$$X_m = -r_p(M)V/F_{m,\text{in}}$$

$$X_{O_2} = -r_{O_2}(O)V/F_{O_2,\text{in}}$$

$$X_{\text{Pr}} = -[r_{t1}(\text{Pr}) + r_{\text{co}}(\text{Pr})]V/F_{\text{Pr,in}}$$

The conversions are defined as,

$$X = (F_{\text{in}} - F_{\text{out}})/F_{\text{in}} \tag{20}$$

for whatever of the species. In the former equations, the volume of a particular CSTR is taken in dm^3! The elemental CSTRs are taken to operate isothermally, at constant pressures (i.e., at the conditions of the inlet streams). The concentrations appearing in the rate equations were taken the same as at the inlet conditions. It is justified by the small particular conversions in the CSTRs, resulting from proper segmentation of the tubular reactor into a large number of CSTRs. Side-injection streams are simply accounted by the equation:

$$(F_{\text{in}})_{j+1} = (F_{\text{out}})_j + F_{ss} \tag{21}$$

Temperature difference between the inlet and the outlet of a CSTR is relatively small and is used to compute the operating temperature of the next CSTR:

$$T_j = T_{j-1} + \Delta T_{L,j-1} \tag{22}$$

A side stream injection point is located between the two adjacent CSTRs, and the next mixing rule is applied:

$$T_{j+1} = (F_{j,\text{out}}T_j + F_{ss}T_{ss})/(F_{j,\text{out}} + F_{ss}) \tag{23}$$

The latest equation is based on the assumption of a constant heat capacity of the reaction mixture along the tubular reactor. Longitudinal temperature difference, ΔT_L, is obtained by the heat balance of elemental CSTR[7,8]:

$$Q = (\Delta h_{m,\text{in}}F_{m,\text{in}} + \Delta h_{p,\text{in}}F_{p,\text{in}} + \Delta H_R^0(F_{p,\text{out}} - F_{p,\text{in}}) + \Delta h_{m,\text{out}}F_{m,\text{out}} + \Delta h_{p,\text{out}}F_{p,\text{out}}) \times 28(\text{J/s}) \tag{24}$$

$$Q = Q_1 + Q_2 \tag{25}$$

$$Q_1 = A_0U_0\Delta T \tag{26}$$

$$Q_2 = \Delta T_L C_p(F_{p,\text{out}} + F_{m,\text{out}}) \times 28 \tag{27}$$

Δh's are the enthalpy differences of monomer and polymer in reference to the standard state.[8] ΔT's of an elemental CSTR are illustrated in Figure 2.

The symbol F_p is used to denote the molar flow rate of the monomer being polymerized. Although the elemental CSTR was assumed to operate iso-

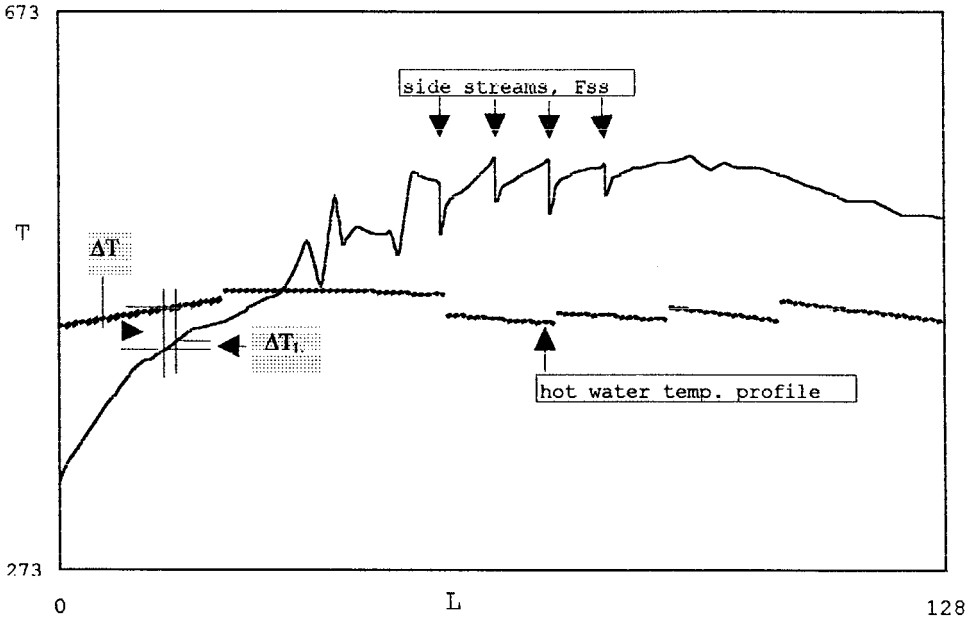

Figure 2 Temperature profiles for run no. 1, ΔT, and ΔT_L definitions in an elemental CSTR; L, length of the reactor expressed in the number of elemental CSTRs.

thermally at the inlet conditions, the outlet pressure is decreased for a finite pressure drop. Namely, total pressure drop along the reactor's tube is equally partitioned between the elemental CSTRs. That is the reason for different specific enthalpies of the species between the inlet and outlet of a CSTR.

Over 98% of the reaction mixture constitute monomer and polymer. The enthalpy calculations are therefore based just on these species.

Two parts in the overall heat effect of the polymerization are distinguished:

1. Heat Q_1 removed through the reactor wall by the temperature difference, ΔT, and
2. Sensible heat Q_2 resulting with a longitudinal temperature difference, ΔT_L, in a CSTR.

The former of these as well as the overall reactor's pressure drop will be better detailed in the second part of this work.

Considering the specific enthalpy of polymerization, ΔH_R^0, different values can be found in the published literature. For the purposes of this work, the value $\Delta H_R^0 = 3900$ J/g was adopted.

POLYMER STRUCTURAL PROPERTIES

In each of the elemental CSTRs, short chain branches (SCB), vinyl ($V1$), and vinylidene ($V2$) indices were determined by the equations given in the master model:

$$\mathrm{SCB} = k_b/(k_p C_m) \tag{28}$$

$$V1 = k_{\beta 1}/(k_p C_m) \tag{29}$$

$$V2 = k_{\beta 2}/(k_p C_m) \tag{30}$$

Number average degree of polymerization, DP_n, is given by,

$$DP_n = 1/(1 - B - C) \tag{31}$$

and weight average degree of polymerization, DP_w, by,

$$DP_w = (1 - B^2 - C^2)/(1 - B - C)^2 \tag{32}$$

Parameters B and C are determined by the equations:

$$B = k_p C_r C_m/D \tag{33}$$

$$C = k_{tp} C_r C_p/D \tag{34}$$

and,

Table IV Reactors and Process Characteristics

Characteristic	R1	R2	R3	R4
Tube diameter (mm)	52	52	52	46
Tube length (m)	1160	1160	1160	800
Pressure range (Mpa)	230–265	230–265	230–265	200–220
Number of zones	7	6	6	3
Throughput (kg/h)	46,000	46,000	46,000	28,500
Conversion range (%)	16–22	16–22	16–22	15–17
MFR range (g/10 min)	0.2–12	0.2–12	0.2–12	0.2–4
Number of side streams	4	4	4	none

$$D = k_p C_r C_m + k_{t1} C_r C_{t1} + k_{tp} C_r C_p + k_t C_r^2 + (k_{\beta 1} + k_{\beta 2}) C_r + C_r/\tau \quad (35)$$

Equations (28) to (35) were taken from the master model. In the case of copolymerization, it was necessary to use modified eqs. (33) and (35):

$$B = (k_p C_r C_m + k_{co} C_r C_{Pr})/D \quad (33a)$$

$$D = k_p C_r C_m + (k_{co} + k_{t1}) C_r C_{pr} + k_{tp} C_r C_p + k_t C_r^2 + (k_{\beta 1} + k_{\beta 2}) C_r + C_r/\tau \quad (35a)$$

The summation along the series of CSTRs is performed by using the mixing theorem,[5] as was demonstrated in the author's earlier article.[9] τ is used for a CSTR's resident time[6] and should be expressed in seconds.

EXPERIMENTAL

Kinetic parameters A, E, and Δv for the processes (E), ($A1$), and ($A2$) were determined by the use of experimental data obtained from four tubular reactors. Oxygen was used in the experiment as initiator; *i*-butane, *n*-butane, and propylene were used for telomerization/copolymerization. Some important reactor features are summarized in Table IV.

The reactors are designated as R1 to R4. Normal production runs of standard film resin types were used for experimental purposes. Temperature profiles for one of the runs are shown in Figure 2.

High-pressure pressure–volume–temperature–enthalpy (PVTH) properties for both ethylene and polymer were computed by the interpolation formulas derived by this author.[7] The reaction mixture was considered an ideal solution[8] of monomer and polymer, the density of which is given by the equation:

$$\rho_{mx} = \rho_e w_e + \rho_p w_p \quad (36)$$

with w_e and w_p expressing the weight fraction of monomer and polymer, respectively. Minor amounts of other constituents were neglected. Concentrations of the pertinent species are then easily computed by the known conversions and density. It should be noted that C_p denotes molar concentration of ethylene being polymerized. Activation energy and volume for the process ($A1$) (i.e., oxygen initiation rate constant k_{O_2}) were assumed to be the same as at Brandolin et al., E = 116,000 J/mol and Δv = 0 cm^3/mol. Corresponding parameters for the initiator effectiveness factor, f, were adopted the same as for micromixing time, t_m, at Lorenzini et al. (Table III). Propylene and *i*-butane telomerization/copolymerization parameters, E and Δv, were taken with unique values, the same as in the master model for *n*-hexane.

Based on the former assumptions, a simulated computer program was made. The set of the input parameters include the following:

- temperature profiles of the reactor
- inlet pressure
- flow rates of the main reactor stream and the side streams
- compositions of the reactor's inlet streams
- flow rates in the hot water system of the reactor's jacket
- inlet and outlet temperatures in the hot water system

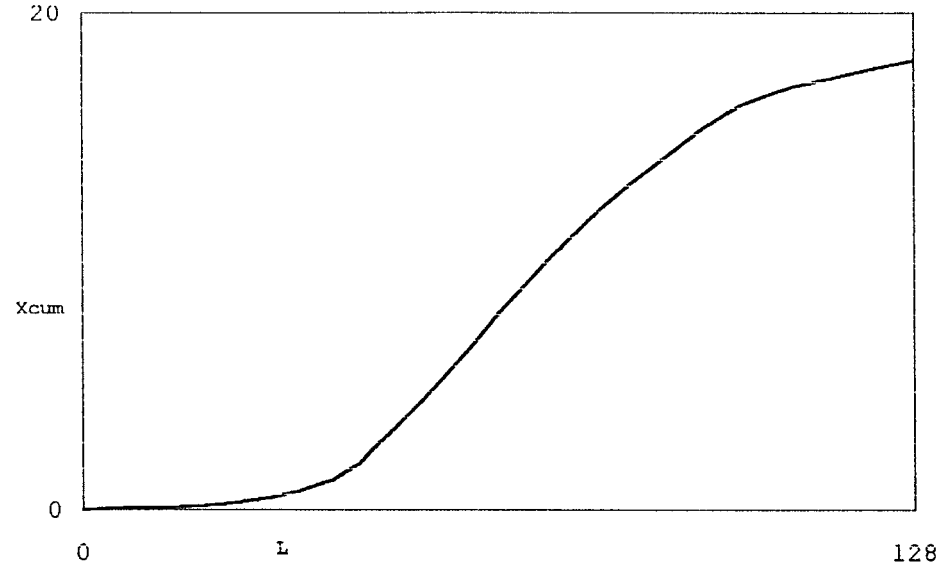

Figure 3 Cumulative conversion, X_{cum}, for run no. 1.

Estimates of the unknown frequency factors, *A*'s, were varied until a satisfactory match between experimental and computed conversions and degrees of polymerization were achieved for each of the runs. Thermal initiation process (*A*2) was then introduced to improve the fit over a broader pressure range. Ten runs totally were used for the model development. Some important features are given in Table IV.

RESULTS AND DISCUSSION

Experimental results are given in Table III. Considering the conversions, the presented model holds within ±6.5% for all of the experimental runs. Better precision can be achieved by a fine-tuning particular reactor. Namely, the errors caused by the model imperfections, instrumenta-

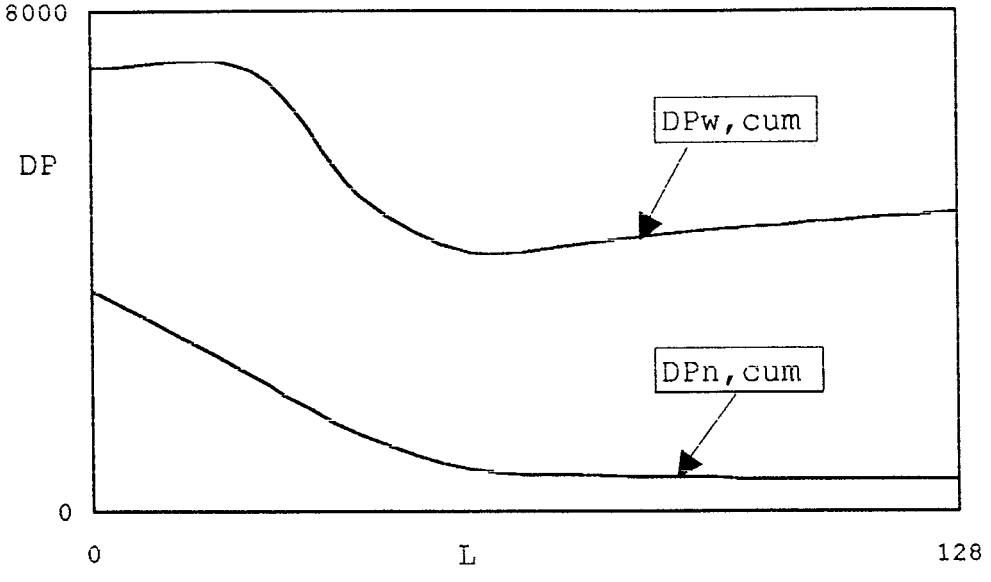

Figure 4 Cumulative degrees of polymerization, DP_w and DP_n, for run no. 1.

Table V Experimental and Computed Results for Run No. 1, Reactor R1

	Experimental	Computed
Inlet pressure (MPa)	253.9	—
Conversion of monomer (%)	18.0	18.1
Conversion of telomer (%)	2.72	2.60
Inlet concentration of telomer (mol %)	0.88	—
MFR (g/10 min)	0.26	0.27
DPn	450	520
DPw	4800	4800
SCB (per 1000C atoms)	28	26
*V*1 (per 1000C atoms)	0.12	0.11
*V*2 (per 1000C′atoms)	0.22	0.28

tion precision, and other sources make fine tuning of the model necessary.

Two of the experimental runs pertained to the smaller reactor *R*4. This reactor used *n*-butane for the telomerization. Kinetic parameters the same as for *i*-butane were successfully applied. However, due to the lack of a more extensive experimental evidence, these are not included in Table III.

Degrees of polymerization, DP_n and DP_w, were determined experimentally by gel chromatography technique for the four of resin types.[10,11] Computed DP_n's deviate approximately $\pm 20\%$ with respect to the experimental values. Because the reproducibility of the experimental determination[12–15] lies in this range, any correction is unnecessary. However, DP_w computations give a considerable underestimate. Therefore, a correction factor $Cf = 1.5$ was introduced into eq. (32).

Equations (28)–(30) for the structural properties, SCB, V1, and V2, hold reasonably well. Experimentally, these properties were determined by IR spectroscopy. Equation (28) gives the uncorrected value for SCB, produced via process (*D*). Because the process (*E*) also produces methyl groups, it should be taken into account.

Comparison of some modeled and actual performances are given in Figures 2–4 and Table V for one of the experimental runs and reactor *R*1. It is interesting to note that the rate constant k_{O_2} determined in this work is quite close to that reported by Ogo.[3]

The model of Lorenzini et al. was also tried to fuse with the kinetic parameters obtained here. Frequency factors *A*'s in the rate constants k_{O_2}, k_{tl}, and *f* were appropriately scaled, and a good fit was obtained, considering the conversions. Further investigation was abandoned because of the complex computation of the structural properties.

CONCLUSION

The terms model and modeling are frequently found in literature, accompanied by the attributes mathematical and/or computer. A mathematical model comprises a set of the mathematical expressions. Modeling, however, denotes an action of the model building or/and model utilization in the computation procedure. Quite generally, model is a functional relation between inputs and outputs. Associated with computers, they found many applications in engineering and manufacturing.[16–18]

This article presents a part of the LDPE tubular reactor model. Its aim was primarily for the reactor control/information system upgrading. Such a system usually includes simulation programs, supervisory programs, real-time data transactions, statistics, etc. The first two of these are model based. Economic benefits of these computer-aided systems were reported.[17]

The simplicity of the mathematical model enables personal computers to be used effectively for an integration with a reactor control and monitoring system. With the aid of the model fine tuning, simulation and supervisory software can be precisely adjusted for a particular reactor. Further model extensions (additional initiators, telomers, and comonomers) are also possible in a simple manner. By this means, the model of Goto et al. is proven to be still useful and effective.

REFERENCES

1. Agrawal, S.; Chang, D. H. AIChE J 1975, 21 (3), 449.
2. Lorenzini, P.; Pons, M.; Villermaux. J. Chem Eng Sci 1992, 47, 3969.
3. Brandolin, A.; Capiati, N. J.; Farber, J. N.; Valles, E. M. Ind Eng Res 1988, 27 (5), 784.
4. Goto, S.; Yamamoto, K.; Furui, S.; Sugimoto, M. J Appl Polym Sci, Appl Polym Symp 1981, 36, 21.
5. Villermaux, J.; Blavier, L. Chem Eng Sci 1984, 39, 87.
6. Fogler, S. H. Elements of Chemical Reaction Engineering; Prentice Hall: Englewood Cliffs, NJ, 1986.
7. Cerinski, B. Polimeri 1995, 16 (2), 56.
8. Smith, J. M.; Van Ness, H. C. Introduction to Chemical Thermodynamics; McGraw Hill: New York, 1975.
9. Cerinski, B. Polimeri 1999, 20 (1–2), 29.
10. Grkovic, V.; Jelencic, J. Polimeri 1987, (10/11), 303.
11. Vrcelj, M.; Maric, N.; Verbanac, R. Polimeri 1990, 11 (3/4), 58.
12. Meissner, J. Pure Appl Chem 1975, 42, 553.
13. Winter, H. H. Pure Appl Chem 1983, 55, 943.
14. Strazielle, C. Pure Appl Chem 1975, 42, 615.
15. Ball, W.; Scholte, T. G. Pure Appl Chem 1978, 50, 1715.
16. Pertsinidis, A.; Papadopulos, E.; Kiparissides, C. Computer Chem Eng 1996, 20, S449.
17. Hydrocarbon Processing: Advanced Process Control Handbook V; 1990, 69 (9), 81.
18. Marquardt, W. Computer Chem Eng 1996, 20, 591.